CMSA project; running blades

Gabriele Decortes, Fabio Marchi, Emanuele Nicolò Pizzo

AY 2024-2025

Contents

Chapter 1

State of the Art

1.1 History of leg prosthesis

The development of prosthetic devices has always stood at the intersection of human necessity and technological advancement. Historical evidence of prosthetics dates back to ancient civilizations, including the Egyptians and Romans, with several examples discovered in mummified remains. At that time, the main purpose of prostheses was largely aesthetic rather than functional. Over the following millennia, progress

Figure 1.1: Egyptian wooden toe prosthesis (ca. 1000 BCE), one of the earliest known prosthetic devices.

remained minimal until the Renaissance, a period of rediscovery in the arts and sciences, when more systematic approaches to prosthetic design began to emerge.

Ambroise Paré, often regarded as the father of modern surgery, played a pivotal role during this period. Not only he refined amputation techniques, but also developed some of the earliest functional lower limb prostheses. These early devices, primarily constructed from iron, were heavy but introduced mechanical articulations such as knee joints, marking the first attempts to replicate natural limb motion.

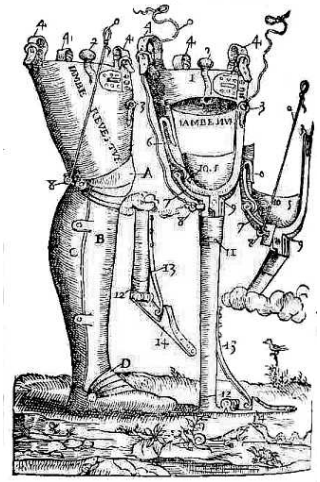

Figure 1.2: Ambroise Paré's prosthetic leg, 16th century.

Despite these early advances, prosthetics remained rudimentary and limited in function. Significant improvements occurred only sporadically, often as unintended consequences of conflict. For instance, the American Civil War in the 19th century resulted in a surge of amputees, which in turn increased demand for prosthetic solutions. While new materials such as wood replaced heavier metals like iron, designs remained basic. The archetype of this era was the peg leg, an inflexible extension meant to provide stability rather than mobility.

A notable development in foot prosthetics emerged in the 1950s with the introduction of the Solid Ankle Cushioned Heel (SACH) foot. This simple yet durable prosthetic design incorporated a cushioned exterior and a rigid internal core to mimic the natural behaviour of the foot during walking. However, the primary focus of prosthetic technology up until this point was to restore basic locomotion, with no capacity to accommodate athletic activities such as running.

Figure 1.3: SACH foot (1950s): rigid core with cushioned heel for basic walking function.

Prosthetic innovation stagnated for nearly two decades following the introduction of the SACH foot. A turning point came in the late 20th century, largely driven by the efforts of two amputees who significantly influenced the trajectory of prosthetic development.

The first and arguably most influential figure was Van Phillips, who lost his leg in a waterskiing accident. Motivated by personal experience and dissatisfaction with existing prosthetic options, Phillips pursued a career in prosthetic design. Drawing inspiration from animals such as cheetahs and kangaroos, he developed the first true running blades, flexible devices that not only enhanced walking, but also enabled running. His work marked a fundamental breakthrough in the design of sport specific prosthetics.

Figure 1.4: Van Phillips wearing an early prototype of his Cheetah prosthesis.

A second influential figure, more notable for his social impact than technological contributions, was Canadian athlete Terry Fox. In 1980, he took part at the Marathon of Hope across Canada to raise funds and awareness for cancer research following his own leg amputation. Although his prosthesis was not optimized for running, his determination and public visibility inspired widespread support and highlighted the need for more advanced, functional prosthetics suitable for dynamic movement.

Figure 1.5: Terry Fox running in the Marathon of Hope.

Thanks to the pioneering efforts of individuals like Phillips and Fox, the field of prosthetics has undergone a dramatic transformation since the 1980s. Advances in material science, biomechanical engineering, and customization techniques have led to the development of high performance prosthetic devices that serve not only everyday users, but also elite athletes, fundamentally redefining the potential of human mobility.

Van Phillips' pioneering work led to the invention of the Flex-Foot® in 1984, the first prosthetic foot constructed from carbon graphite. Unlike conventional prostheses, the Flex-Foot was engineered to store and return energy: it would deform elastically upon ground contact and release that energy during toe-off, allowing for a more dynamic and efficient gait. Later, the introduction of carbon fiber laminates marked a turning point in prosthetic design. These composites offered customizable stiffness, high durability, low weight, and superior responsiveness, far surpassing earlier metal or polymer-based devices.

The first competitive use of the Flex-Foot in elite sports occurred at the 1988 Seoul Paralympic Games, and subsequent iterations, such as the Flex-Sprint I, introduced significant modifications for sprinting, including the removal of the heel and the adoption of a curved J-shape to better replicate forefoot running dynamics. This evolution laid the foundation for modern running specific prostheses (RSPs), like the iconic "Cheetah" (Össur, Iceland), introduced in 1996.

Figure 1.6: Example of Cheetah prosthesis.

Today's running blades are highly sophisticated devices, often composed of over 90 layers of unidirectional carbon fiber, each thinner than a human hair. Each blade is customized based on the user's weight, running style, and specific discipline. Sprinting blades tend to be stiffer for rapid energy release, while endurance versions allow greater flex to minimize fatigue over long distances.

Phillips' approach was revolutionary not only for material selection, but also for its bio-inspired philosophy. Rather than mimicking the anatomical shape of a leg, he drew from the biomechanics of animals such as kangaroos and cheetahs and sports movements like diving and pole vaulting. This shift from anatomical replication to mechanical optimization has since defined modern prosthetic design. The impact of these innovations has been profound. In the T44 sprint category (single below-the-knee amputation) , for instance, the integration of RSPs led to performance improvements of up to 1.5 seconds in the 100 meter dash within a decade. American sprinter Tony Volpentest notably lowered his time from 14.38 seconds in 1989 to 11.36 seconds by the 1996 Atlanta Paralympics after transitioning to Flex-Foot technology.

These advancements have blurred the lines between able bodied and para-athletic competition. The case of Oscar Pistorius, who competed in both the Paralympic and Olympic Games in 2012, sparked a global debate on the potential advantages of carbon fiber blades. This discussion has prompted extensive biomechanical studies on energy return, ground contact time, and running economy, fuelling ongoing research into equitable and high-performance prosthetic design.

Meanwhile, parallel improvements in socket systems, suspension mechanisms, and even sensor-based feedback have enhanced the safety, comfort, and performance of lower limb prostheses. Innovations such as vacuum suspension and adjustable alignment have improved proprioception and reduced the risk of injury during intense training.

In sum, running specific prostheses today represent the convergence of materials science, biomechanics, and human resilience. They enable athletes not just to participate, but to excel—often rivalling their non-amputee peers. More broadly, they reflect a cultural shift that sees disability not as a barrier, but as a powerful catalyst for innovation and achievement.

1.2 Structure and materials

Running Specific Prosthesis (RSP) were created to allow amputees to take part in sport activities without the limitations that their disability implied. Developing a RSP is an easier task than designing an "all-around" prosthesis that could adapt to different situations, because it is easier to imitate the behaviour of a joint or limb during one specific activity rather than modifying a Daily-Use prosthesis.

The main challenge in running prosthesis design is the achievement of a good cooperation between athlete and leg during physical activity. The most complex aspect is the will of the amputees to have complete control over their limb: in order to allow a better functioning of the man-machine system, there must be a direct link between the physiological system and the movement of the artificial limb.

RSPs are made up of three main components.

1.2.1 Liner

It is a cap that holds and protects the stump; it limits relative movements between the skin and the rest of the prosthesis (to avoid friction and thus tissue damage) and prevents concentrated stress points, making uniform the pressure and forces that form during exercise. It can be made in silicon (best for small mobility activities) or polyurethanes (easy to adapt to different requirements).

Figure 1.7: Liner of a prosthesis.

1.2.2 Socket

It is the most important part of the artificial leg, since it is the component that effectively allows the control of the prosthesis and minimizes energy loss. It is custom made for athletes because every stump has a different shape and dimension, and can be of two types:

- *Rigid socket*: light structure made in polypropylene
- *Flexible socket*: it consists in an internal polyethylene socket (low friction coefficient, transparent, flexible) inserted in a carbon fibre frame; this type of socket is much more comfortable, as it adapts to the movements and deformations of the stump that happen during the activity.

To achieve a better connection with the stump, low weight and low thermal exchanges are necessary: new developments in smart materials (ex. phase-change) will lead to more connected sockets.

Figure 1.8: Socket of a prosthesis.

1.2.3 Blade

Usually produced in carbon fibre, it is the part that mimics the elastic behaviour of calf muscles and ankle. Its function is to act as a spring that transmits the energy from the stump to the ground.

The shape of the blade is the parameter that contributes the most to the runner's velocity and depending on the sport, type of amputation and specific needs of the athlete, the available products can be several (both commercial and custom made), but two main shapes are used:

- *"C" shape*: mostly used for jogging or distance running.
- *"J" shape*: better spring efficiency, thus used more in sprinting or jumping.

(a) C-shape. (b) J-shape.

Other components may be added, depending on the state of the limb or activity:

- *A tubular structure* that compensates the height of the missing leg; the materials most fit to this component are titanium or aluminium alloys
- *A prosthetic knee* that allows for better control of the blade and adapts to the velocity and running style of the athlete
- *A rubber pad* added on the segment that touches the ground; this increases traction and shock absorption.

1.2.4 Running blade

Although glass fibre has been used in the past and is still being studied today, carbon fibre remains the best material for blade construction, due to its overall better properties. Energy absorption, deformation and strength are the main parameters considered in tests, and carbon fibre blades have led to better results compared to glass fibre.

A running athlete can be modelled as a spring-mass system, with the mass representing the entire body and the spring representing the leg or blade. In this model the leg is assumed to be completely elastic, but in reality legs are a viscoelastic element: even though some energy is necessarily lost through hysteresis, a significant portion of the runner's energy is preserved, allowing for an efficiency of almost 240% (mostly thanks to the ankle joint). Running blades nowadays can only return up to 90% of energy, so it is obvious that, even after 40 years from their original prototype, there is still a large margin of improvement.

Figure 1.10: Example of prosthesis used at the highest stage.

1.3 Design and Manufacturing

1.3.1 Preliminary process and fibers disposition

The production of a running blade starts from the patient to guarantee a high level of personalization. A preliminary step involves the use of CAD/CAM technologies to create sockets that precisely match the patient's residual limb and that perfectly attach to the blade. The socket design ends when the measurements and requirements from the patient are collected and, only then, the proper manufacturing of the blade starts. A FEA[1] is performed on the structure to ensure that the component won't fail in any way during its life, and the model correlation is performed to confirm the validity of the FEA.
In terms of composite material design, literature shows two different trends.

- *Use of "2D" laminates (CLT [2])*; the blade is composed of 50 to 90 layers of unidirectional laminae. The disposition, stacking and direction of each ply is optimized to withstand certain loads (fig. 1.11).

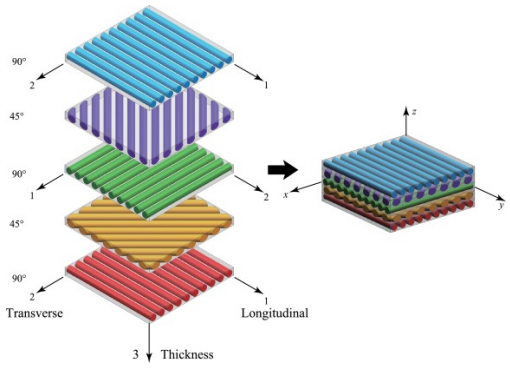

Figure 1.11: The concept behind the classical lamination theory; stacking unidirectional layers to obtain multiple-direction properties.

- *Use of 3D-woven fabrics*; two dimensional fabrics are interconnected by a z-yarn to avoid delamination under specific loading conditions. The control of the path of the warp binding yarns allows not only the design of stiffness in two principal axial directions, but also in one out-of-plane shear axis [6] (fig. 1.12).

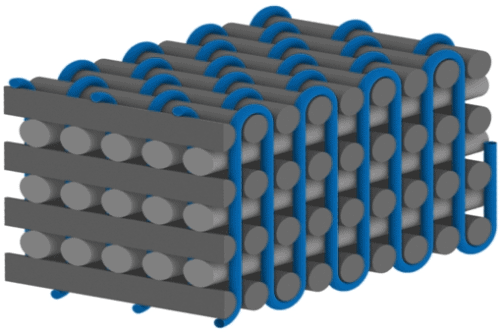

Figure 1.12: 3D woven composite.

Depending on the fibers disposition, the manufacturing method can change; for this reason, in this work we will focus on 2D laminates.

1.3.2 Classical manufacturing methods

- *Hand lay-up*: The resin is manually infused into fabric fibres that are woven, weaved, stitched, or bonded. Modelling is the initial step in this technique. Once poured, the resin is evenly dispersed across the fibre substrate; this is usually done with the use of rollers that also press the resin onto the

[1] Finite Element Analysis
[2] Classical Lamination Theory

fabric. Then, with a brush, the trapped air in the layer is removed and curing of the laminate begins. It is an open mould process [7] (fig. 1.13).

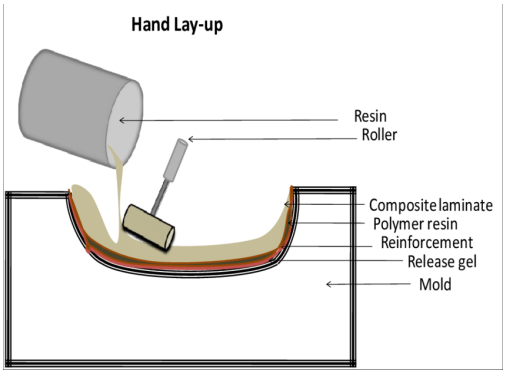

Figure 1.13: The Hand Lay Up system

- *Prepreg Vacuum bagging*: the composite material is supplied by an external manufacturer as prepreg, meaning the fibers are pre-impregnated with the correct resin-to-fiber ratio. The process begins by applying a release film onto the open mould surface to ensure easy detachment of the final component from the mould. Next, a peel ply is placed over the release film to confer a better surface finish and facilitates potential secondary bonding operations. The prepreg sheets are then cut properly and carefully laid onto the mould. A roller is used to conform the layers to the mould surface and eliminate air pockets, ensuring good compaction prior to the vacuum bagging and curing steps. The vacuum pump both extract excess resin and evacuate gases during the curing process (fig. 1.14)

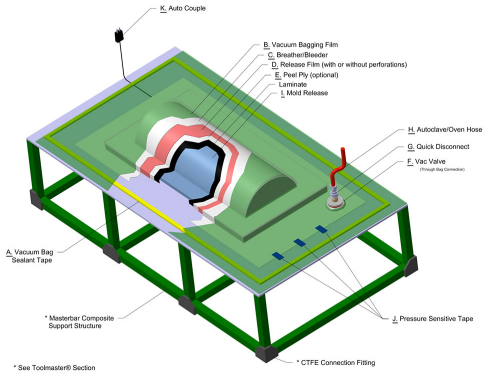

Figure 1.14: The Prepreg Vacuum Bagging system

- *Resin Transfer Moulding (RTM)*: the resin is injected under pressure into the mould cavity where dry reinforcement materials are already placed. This method, even if rarely used, provides flexibility to the combination of fiber orientation. Since the process is performed in vacuum, there is no need to brush air pockets in the end. It provides flexibility, fast cycle times and allows the combination of materials and their orientation, including 3-D reinforcements [7] (fig. 1.15).

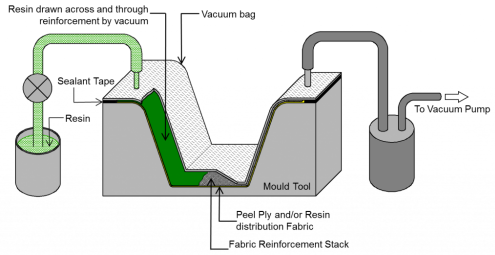

Figure 1.15: The RTM system: it is a close mould process and, as for hand lay up, a gel coat is applied to guarantee suitable surface finish.

1.3.3 Innovative manufacturing methods

3D printing of fiber-reinforced thermoplastic polymers is being investigated in several studies. Among various types of polymer composites, Nylon reinforced with carbon fiber is among the most popular with a wide range of applications. Some case studies of running blades reported sufficient mechanical properties of the structure manufactured through additive manufacturing (AM) technologies; however, process-related problems are well present in today's systems. In particular, 3D printed continuous and aligned fibers composites are limited in terms of design freedom, as fiber placement is challenging and more voids are created, especially when printing complex shapes. Design freedom is one of the main advantages of AM over conventional manufacturing, and incorporating continuous fibers into the matrix through 3D printing negates this advantage.
Three methods are used to embed fibers into the matrix [5].

- *Prior incorporation*: the treated fibres and polymer matrix are mixed and then fed into an extruder. The composites normally go through the second extrusion process to obtain better matrix distribution and reinforcement.

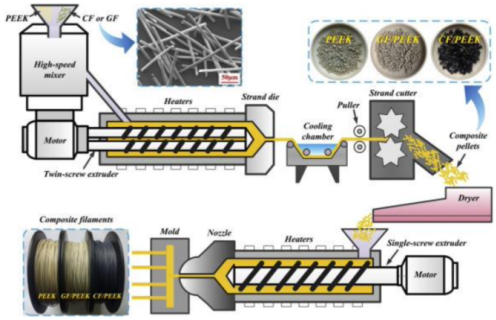

- *Incorporation in the nozzle*: both polymer matrix and reinforcing fiber are mixed in the nozzle during the printing process, requiring two material supplies. The extrusion nozzle receives both the thermoplastic polymer and the continuous fiber; when the nozzle is heated, infusion of the matrix occurs and the molten thermoplastic material is deposited along with the reinforcing filament.

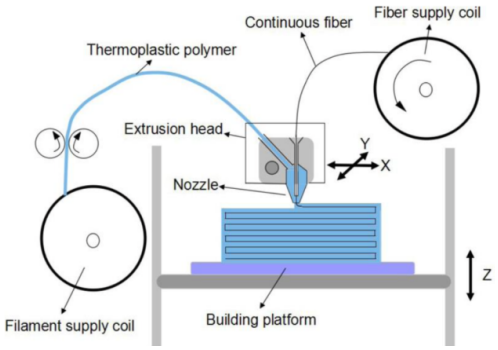

- *Incorporation on the component*: composites produced by this method require two or more independent extruders, each with an independent nozzle, to deposit both polymer matrix and reinforcement fiber on the component.

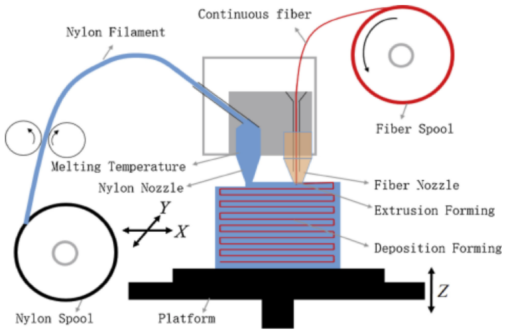

Chapter 2

Discussion and results

2.1 Problem statement and objectives definition

The purpose of this work is to design a J-shaped running blade intended for short-distance Paralympic competitions, such as the $100\,m$ and $200\,m$ sprints, by employing and comparing composite materials and light alloys.
In particular, our blade is based on the "Cheetah Xtreme" model by Össur. The theoretical framework of this project is the Classical Lamination Theory; as such, the component is composed of a sequence of unidirectional laminae, the plies, which were strategically arranged to optimize the blade's performance.
The optimization process followed several steps, as outlined below.

Structural Integrity Check

The first step was to ensure structural integrity under a load of $2000\,N$, a typical force experienced by the blade during competition [8]. To accomplish this, the Tsai-Hill failure criterion was employed for the composite materials, while the von Mises criterion was used for the metallic alloy.

Figure of Merit Definition and Material Optimization

Once the minimum thickness and number of plies required to guarantee structural integrity were identified, the optimization phase began. This step aimed to determine, for each material, the minimum thickness that ensured a maximum tip displacement of $4\,cm$. This displacement limit corresponds to a target structural stiffness of $50\,N/mm$, as reported in [4], and is derived from the linear relationship:

$$K = \frac{F}{\delta} \tag{2.1}$$

where δ is the tip deflection and F is the applied load.
Optimizing displacement is crucial not only for structural safety but also for athletic performance. Excessive deformation can lead to energy losses, reduced stride efficiency, and diminished propulsion, key factors in sprinting. Therefore, controlling the blade's flexural response is as important as ensuring its strength.

Steps for Objective Accomplishment

To achieve the design objective, a preliminary and simplified analytical model was developed to identify the most critical region of the blade, providing a basis for a more detailed finite element simulation conducted in Abaqus/CAE (Dassault Systèmes), with a detailed evaluation of the stress distribution and deformation characteristics of the blade under load.
Once a configuration satisfying both failure and displacement criteria was identified, the final step involved comparing the total weight of the blades. This parameter is critical, as reducing the inertial mass of the limb significantly enhances performance. The lightest viable configuration was ultimately selected.
This study thus presents a comprehensive methodology that combines mechanical modelling, finite element analysis, and material selection to develop a high-efficiency running blade tailored for elite sprinting applications.

2.2 Shape definition and analytical model

We created our running blade through SolidWorks (Dassault Systèmes, France), employing dimensions found in ([1], [2]).
First, the lateral profile was sketched: the rear curvature was created by joining two arcs of different radius and the foot was created using a line spline function. The tip of the prosthesis was slightly lifted from the ground, allowing for a better rolling motion (mimicking the "heel-to-toe" movement of the foot) and more energy release in the last part of contact.
The profile was then extruded in the orthogonal direction to achieve the width of the blade. The final result was turned into a shell-type solid using surface-based functions to allow the correct implementation of properties in Abaqus/CAE. The final result is shown in (fig. 2.1.b).

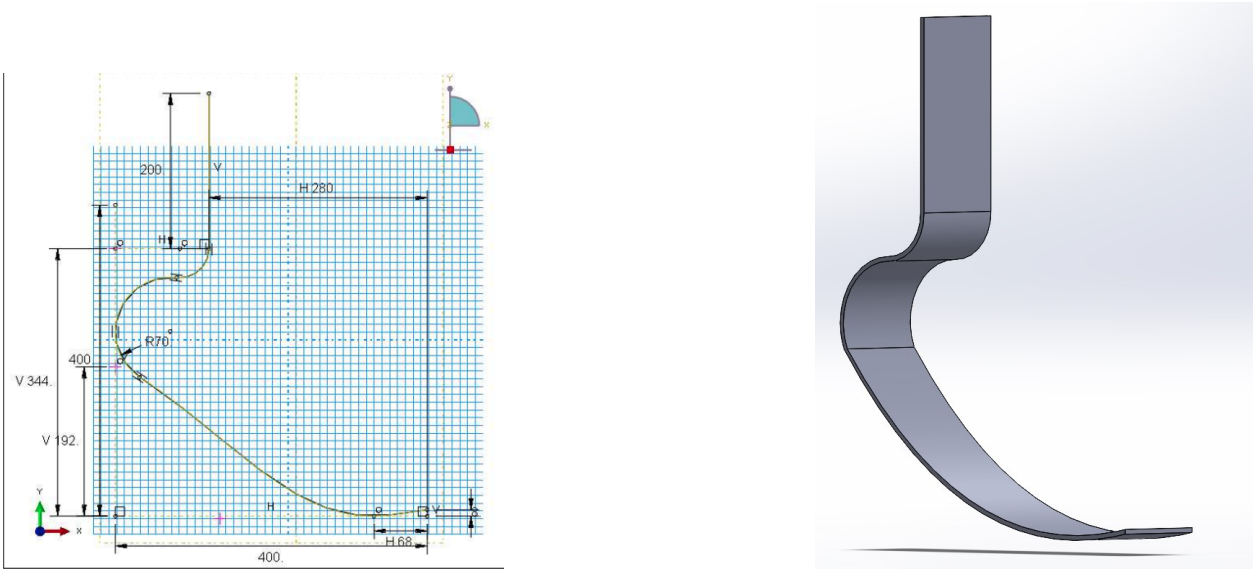

(a) (b)

Figure 2.1: The lateral dimensions of our running blade (a) and the final 3D model (b).

2.2.1 Analytical model definition

Our simplified analytical model consists in a beam system in a 2D plane since, due to symmetry in width, the main effects of stresses and forces can be seen on the profile (fig. 2.2.a). Assuming the contact with the ground as a vertical force F applied on the outer edge of the "a" beam, and considering the top edge of the "e" beam as an encastre (point of connection to the stump), the resulting bending moment diagram was obtained (fig. 2.2.b).

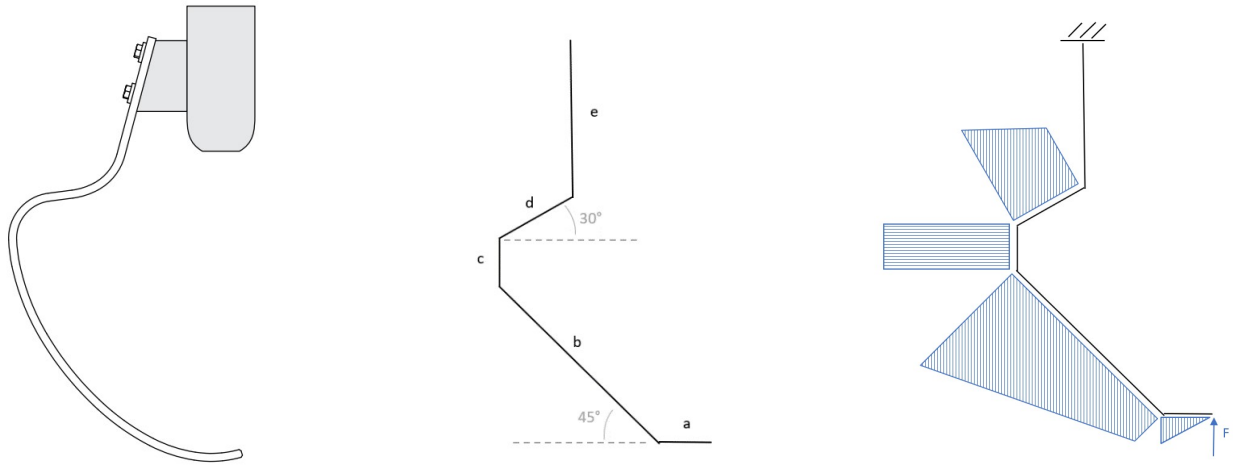

(a) (b) (b)

Figure 2.2: Simplifying process of a running blade (a), (b). Internal bending moment diagram (c).

As a consequence, we expect the most stressed part to be the curved region of the blade, where the quick change in geometry represents a stress concentration region.

2.3 Implementation in Abaqus/CAE

To achieve the objectives of the project and obtain reliable results, a FEA[1] was performed using Abaqus / CAE.
Since two different fiber-reinforced composite materials were investigated, the general modeling and optimization procedure are first outlined, followed by a detailed analysis of the results obtained for each material. The steps concerning the metallic alloy are omitted, as it falls outside the primary scope of this study.

Part module

At first the SolidWorks model was imported into Abaqus/CAE: given that our blade is a solid body with a very small thickness compared to its length and width, we approximated its behaviour as the one of a shell, while still being defined using solid elements. A partition was generated using a custom plane to define the load application area. (fig. 2.3).

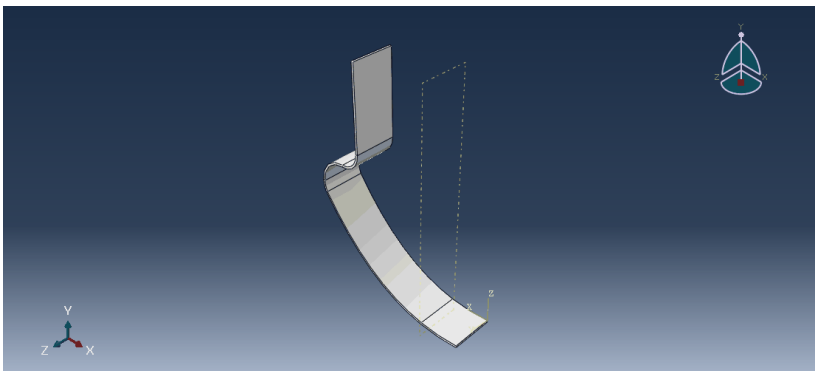

Figure 2.3: The part module of our running blade: the dashed yellow line is the plane used to create the partition.

Property module

The material properties were defined in the Property section. Within the same section, the composite layup of the laminate was specified by detailing the thickness, region, material, and orientation of each individual ply. Since composite laminates are inherently anisotropic, it was also necessary to assign a coordinate system (CSYS)[2] to define the longitudinal direction of the fibre (that is, direction 1) and the stacking direction (that is, direction 3).

To investigate the influence of stacking sequence and fibers orientation on mechanical performance, we defined two initial 20 plies symmetric laminates (eq. (2.2)), (fig. 2.4).

$$[0°, 45°, -45°, 90°, *, 0°, 0°, 90°, -45°, 45°, *, 0°]_S \quad [0°, 45°, -45°, 45°, *, 0°, 0°, 45°, -45°, 45°, *, 0°]_S \quad (2.2)$$

[1] Finite Element Analysis
[2] Coordinate System

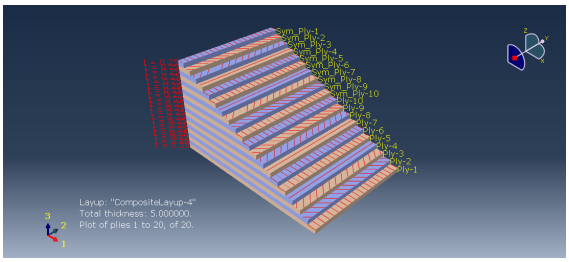

(a)

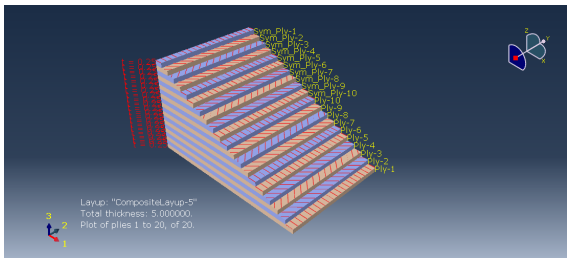

(b)

Figure 2.4: The two initial stacking sequences: (a) is a $[0, 45, -45, 90, 0, 0, 90, -45, 45, 0]_S$ laminate, while (b) is a $[0, 45, -45, 45, 0, 0, 45, -45, 45, 0]_S$ laminate. On the bottom-left corner the CSYS is visible.

We chose stacking sequence (fig. 2.4.a) based on the idea of ensuring reinforcement along the primary structural directions, direction 1 (through 0° plies) and direction 2 (through 90° plies) while providing adequate in-plane shear resistance (through $\pm 45°$ plies): stacking (fig. 2.4.b) was chosen to investigate the influence of the 90° oriented fibers. In fact, we considered this orientation as potentially embrittling, as it does not align with the direction of maximum fiber strength relative to the applied load.
Previously verified that none of our composite materials can withstand the applied load in these configurations, we decided to add plies on the "*" spots in (eq. (2.2)) following this pattern.

- *Stacking (a)*: addition of $[45°, 90°]$ packets.
- *Stacking (b)*: addition of $[\pm 45°]$ packets.

The materials selected for our job are epoxy resins reinforced with two different fibers at $V_f = 60\%$, whose properties are resumed in the following tables.

CFRP

Property	Value
ρ	$1.6\, g/cm^3$
E_1	$177\, GPa$
E_2	$10.8\, GPa$
ν_{12}	0.27
G_{12}	$7.6\, GPa$

(a)

Property	Value
X_f	$3530\, MPa$
X'_f	$800\, MPa$
Y_f	$40\, MPa$
Y'_f	$100\, MPa$
S	$90\, MPa$

(b)

Table 2.1: CFRP properties: table (a) shows the elastic properties of the single ply, while table (b) shows the limit stresses employed in the Tsai-Hill criterion

GFRP

Property	Value
ρ	$1.6\, g/cm^3$
E_1	$43\, GPa$
E_2	$8.9\, GPa$
ν_{12}	0.27
G_{12}	$4.5\, GPa$

(a)

Property	Value
X_f	$1080\, MPa$
X'_f	$620\, MPa$
Y_f	$39\, MPa$
Y'_f	$128\, MPa$
S	$89\, MPa$

(b)

Table 2.2: GFRP properties: table (a) shows the elastic properties of the single ply, while table (b) shows the limit stresses employed in the Tsai-Hill criterion.

AA7075

Because metals are isotropic, different properties were implemented in the software.

Property	Value
ρ	$2.8\,g/cm^3$
E	$72\,GPa$
E_2	$10.8\,GPa$
ν	0.33
σ_y	$500\,MPa$

Table 2.3: AA7075 properties: the table shows both the elastic properties of the alloy and the yielding strength for the Von Mises failure criterion.

At this point, we created the assembly and defined a "static general" step to perform the static assessment of our blade.

Load module

Before evaluating which of the two sequences better satisfied the design constraints, appropriate boundary conditions and loads were applied. The $2000\,N$ load was uniformly applied as a $0.2\,MPa$ pressure on the lower tip surface of the blade (defined by the previous described partition, with an area of $10000\,mm^2$) to simulate ground contact forces during sprinting. The proximal end of the blade, corresponding to the socket attachment point, was fully constrained through an encastre to replicate the fixed interface with the athlete's leg (fig. 2.5).

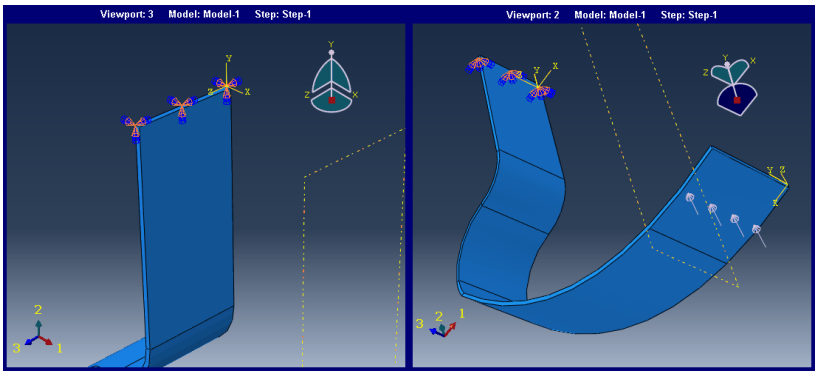

Figure 2.5: Loads and constraints in our model.

Mesh module

The mesh was generated with emphasizing consistency and the logical distribution of elements across the blade geometry. Although the full mesh convergence was not the purpose of this study, we started with a fine mesh of 5000 elements and subsequently reduced it to 2140, which showed a low variation in simulation accuracy (fig. 2.6). We selected a S4R element type, a quadrilateral shell element with reduced integration, and the chosen meshing strategy is "structured" everywhere except the upper rectangle, where the simple geometry and lower interest led to a "free" strategy.

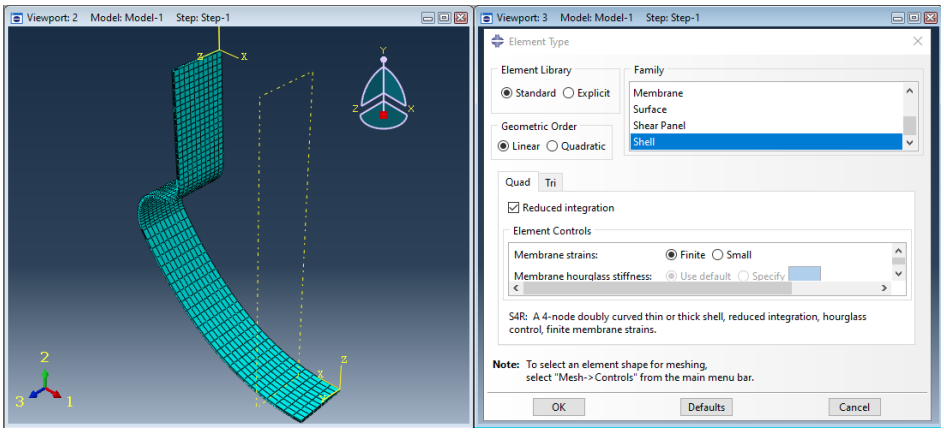

Figure 2.6: The mesh of the blade: note that the elements are not evenly distributed but, conscious of the most critical region of the prosthesis, we decided to rise elements density in the "S" region.

Field output creation and workflow

Once our model was implemented in Abaqus, we defined the output variables for the jobs we submitted. As already specified in (section 2.1), the first step of our work is to determine the minimum number of plies required for each configuration to satisfy the Tsai-Hill failure criterion, identified as "TSAIH" in the Abaqus field output. The optimisation process is carried out by incrementally increasing the number of plies in both base stacking configurations (fig. 2.4) and monitoring the Tsai-Hill failure index F.I. The safety condition is:

$$F.I. \leq 1 \tag{2.3}$$

The optimal configuration is defined as the one that meets the Tsai-Hill criterion with the minimum number of plies.
Subsequently, we verify whether the selected laminates also meet the displacement constraint of $4\,cm$, changing the field output request from "Composite Layup" to "Whole Model". If this condition was not satisfied, additional layers were incrementally added, following the pattern described in (section 2.3) until we met the displacement requirement.
This procedure was repeated for both composite materials and, once the target displacement was reached, we selected the material that guaranteed the lowest weight, a critical parameter in high-speed athletic applications, where reducing inertial mass directly enhances performance.

2.3.1 Results for the blade made of composite material

A first analysis, shown in (fig. 2.7), was done on the maximum stress felt by the blade: from the simulation we confirmed that the most stressed region was the "S"-shaped one.

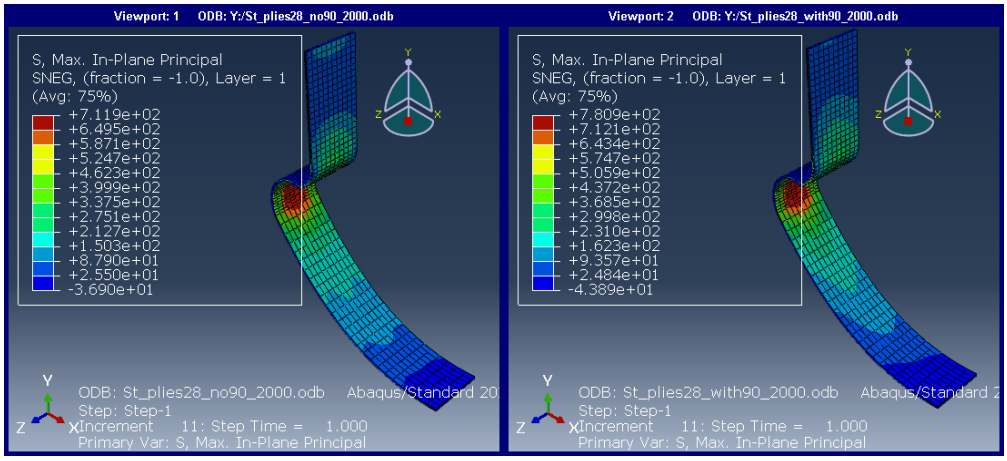

Figure 2.7: In-plane principal stress for the CFRP laminate. The same result can be seen for the other materials, whose magnitude depends only on the thickness of the blade.

Number of plies to avoid failure

Figure 2.8 shows the results for the CFRP laminate.

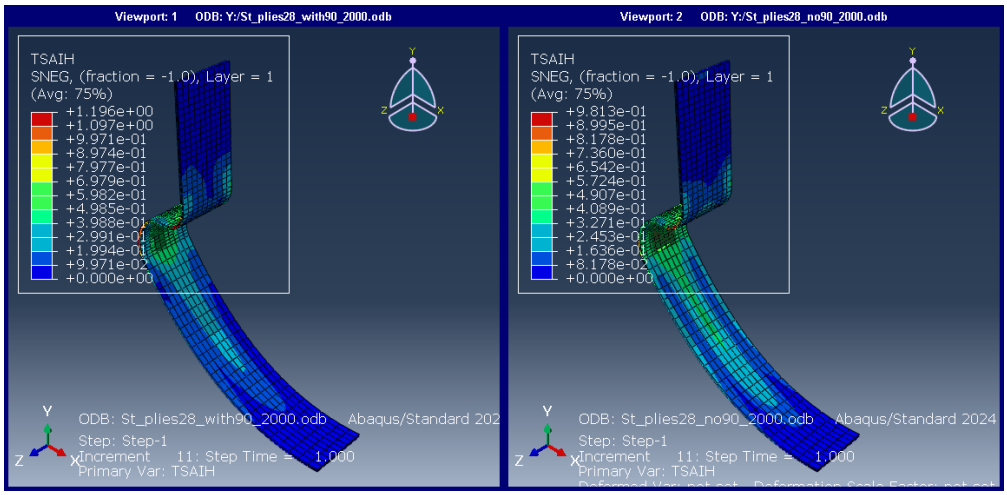

Figure 2.8: TSAIH output for the CFRP laminate.

As shown, for the same number of plies, the failure index of the laminate without 90° plies is approximately 0.98, while the laminate including 90° plies reaches a value of 1.2. This result is obtained with 28 layers. Similarly for GFRP, (fig. 2.9) we observed that the laminate without 90° plies performed better, requiring 44 layers to meet the failure criterion.

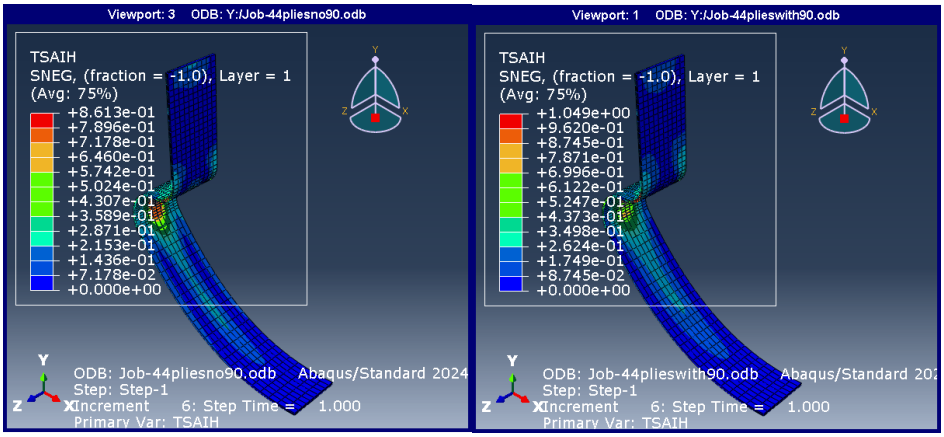

Figure 2.9: TSAIH output for the GFRP laminate.

From the above results, we can state that CFRP laminate reaches a failure index value below 1 with less plies with respect to the GFRP blade.
In conclusion, we can state that, for our application, fibers oriented at 90° are detrimental. This effect is also evident when analysing the strains along direction 1 (E11)(fig. 2.10).

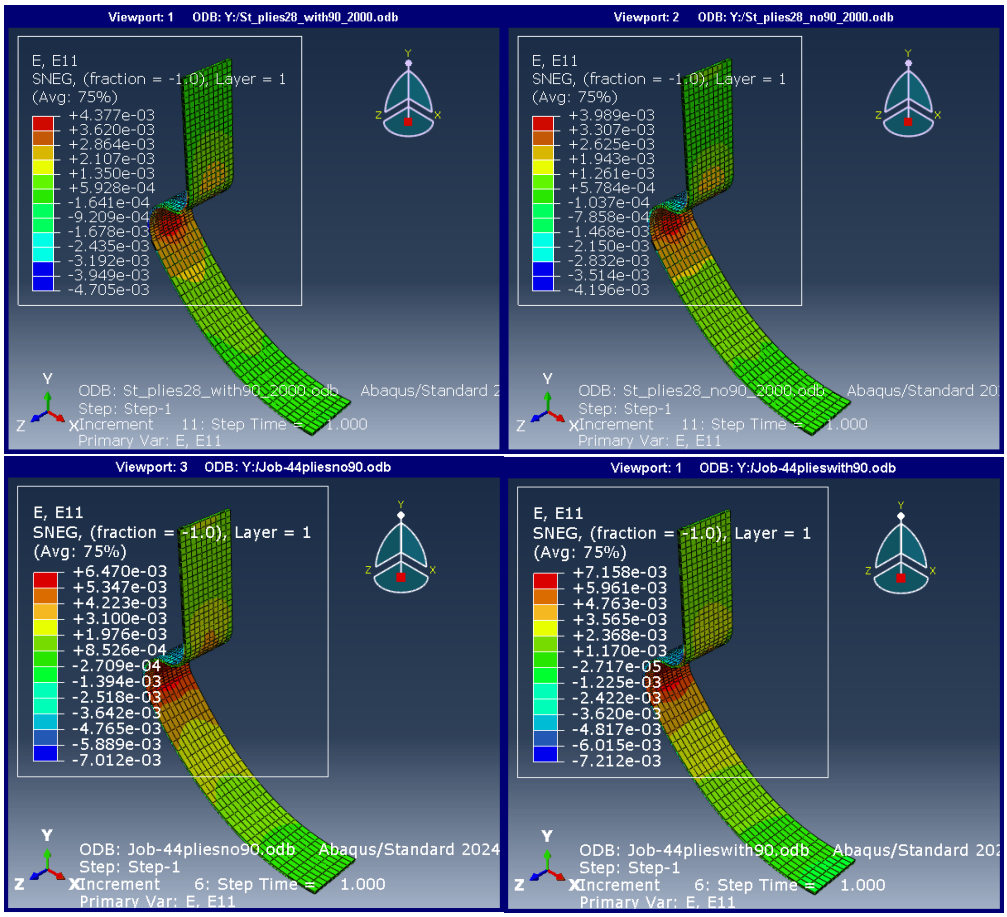

Figure 2.10: Longitudinal strains along 1 direction for the CFRP and GFRP laminates respectively.

E11 values were lower for laminates without 90° layers, a consequence of the fact that the elastic modulus in direction 1 is way higher than Young Modulus in direction 2, resulting in less deformation.

Number of plies for the displacement target

The previous results are a good starting point to reach the optimal performance: however, if we look at the foot tip displacement in direction Y, we note that an excessive value is obtained employing the 28 and 44 plies configurations(fig. 2.11).

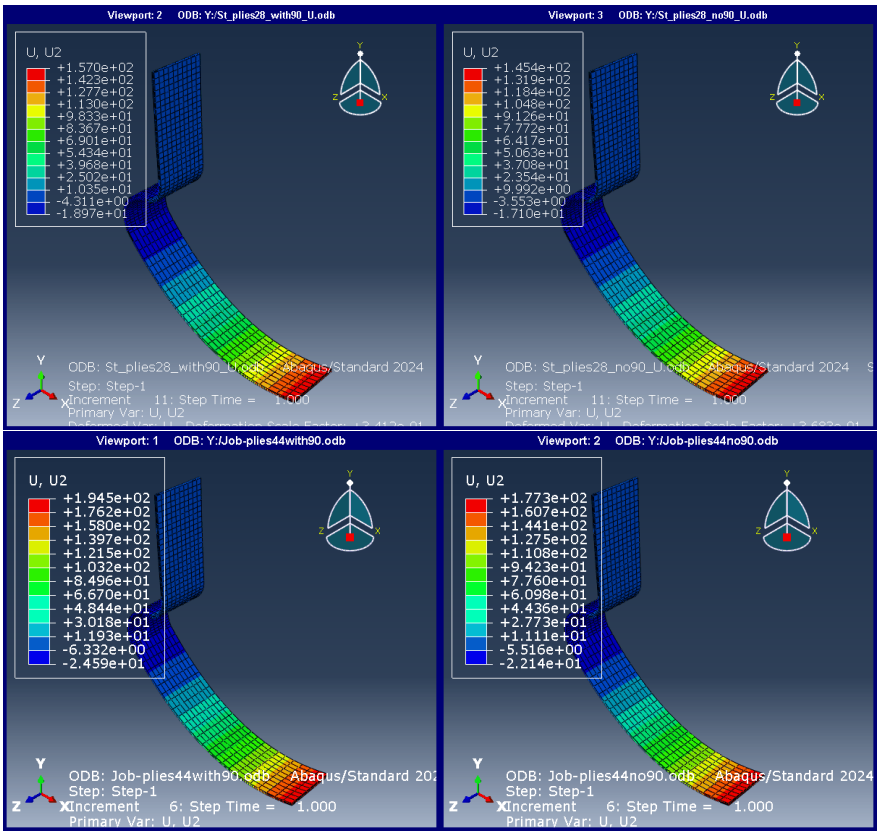

Figure 2.11: A comparison of CFRP and GFRP tip displacement considering the Tsai-Hill based laminates.

For this reason, we proceeded adding plies (still following the pattern presented in section 2.3). The results are presented in the following figures.

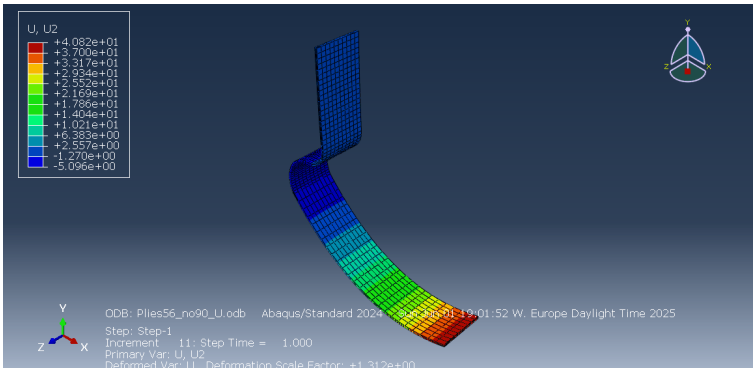

(a)

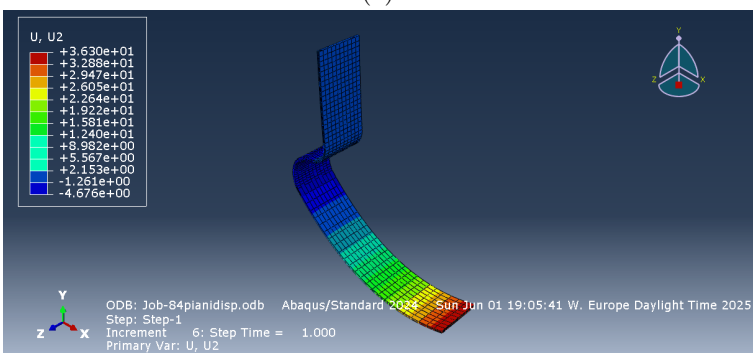

(b)

Figure 2.12: Tip displacement employing a CFRP laminate (a) and a GFRP one (b)

As shown, the target tip displacement of $4\,cm$ was successfully achieved: (fig. 2.12.a) indicates that CFRP reaches this limit with 52 plies, while GFRP requires 84 plies (fig. 2.12.b). Considering a ply thickness of $0.25\,mm$, the total thickness of the CFRP blade is $1.3\,cm$, whereas the GFRP blade reaches $2.1\,cm$.

Chosen material

The simulation results showed that the CFRP blade is $1.3\,cm$ thick, with a volume of $1089\,cm^3$, while the GFRP one is $2.1\,cm$ thick with a volume of $1717\,cm^3$. Because CFRP has a density of $1.6\,g/cm^3$, its blade weights $1.75\,kg$, while the GFRP blade, having a density of $2\,g/cm^3$, weights $3.5\,kg$, making CFRP the best choice for our purpose.

2.3.2 Results for the blade made of AA7075

The same analysis was conducted also for the AA7075 alloy and it showed that the allowed tip displacement could be obtained through a thickness of $1.2\,cm$.

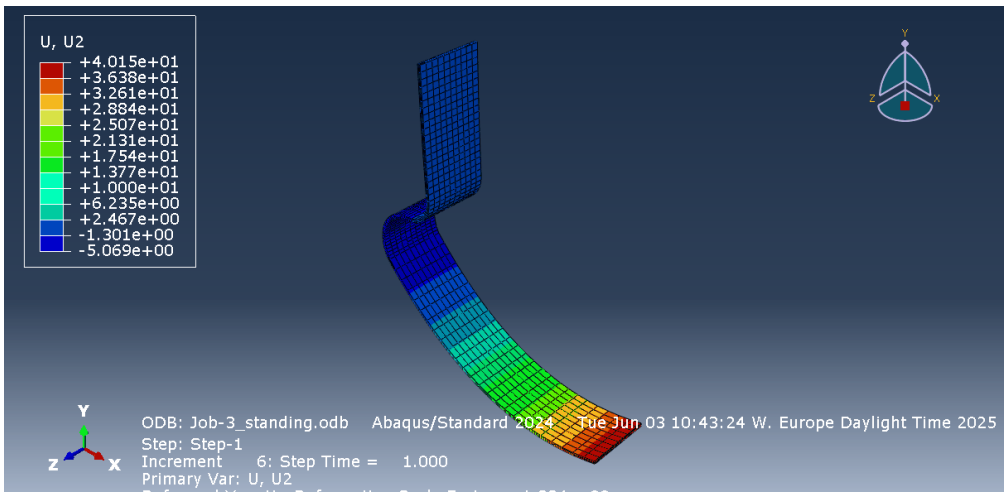

Figure 2.13: Displacement map for the AA7075 running blade.

Therefore, with a volume of $1005\,cm^3$ and a density of $2.8\,g/cm^3$, the AA7075 blade weights $2.8\,kg$.

2.4 Cost evaluation and manufacturing process

Production and manufacturing of objects made of composite materials are not cheap processes: the cost evaluation of the whole process must take into account the cost of raw materials, resin and fibers, manpower, transportation and the power required to operate the production facilities.
An approximated cost evaluation was conducted for the chosen materials and the chosen processes. The following list shows the cost/kg of the raw materials, while fig. 2.14 the overall cost of the optimised blades without considering manufacturing.

- CF: 25 €/kg [3]
- GF: 2 €/kg [3]
- Epoxy resin: 16€/kg
- AA7075: 19€/kg

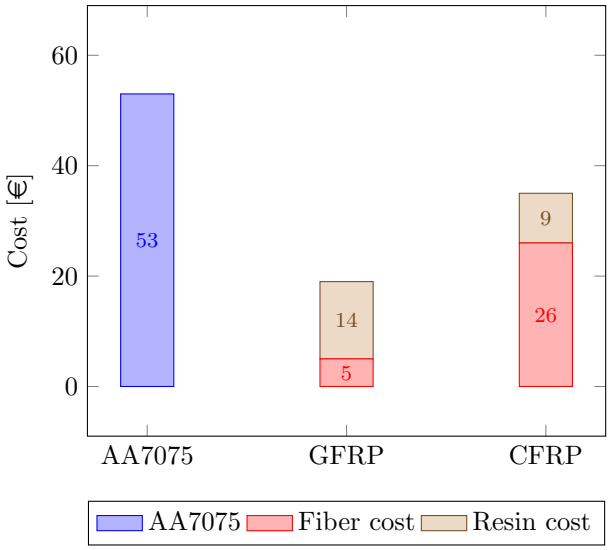

Figure 2.14: Comparison of material costs per blade

From the histogram it is clear that the best performing material is at the same time the most expensive, reaching a cost of 35€(raw materials only). This sensible difference lies on the production process of the two fibers and of the aluminium alloy: CF are produced through the PAN process, where high energy consumption coming from high operating temperatures ($\approx 3000\,°C$) and pre/post treatments rise the price significantly. On the other hand, GF are produced at lower temperatures ($\approx 2000\,°C$) and require only sizing as post treatment, while AA7075 undergoes foundry processes and thermal treatments. The result of these differences is that GF blade costs $\approx 46\%$ less than CF while AA7075 is $34\,\%$ more expensive than CF.
To these costs, we now need to add the machining processes for the aluminium alloy and formability processes for the composites material. For the purpose of this course and for the absence of literature, we decided to avoid the cost evaluation for the aluminium.
Among the manufacturing techniques presented in the state of the art for the production fiber-reinforced composites laminates, RTM and Hand Lay-Up were excluded for this application. RTM, while capable of producing high-quality parts, involves complex tooling and high process costs that are unjustified given the low production volume.
Hand lay-up, despite being cost-effective and simple, is subjected to high variability depending on manpower, leading to non-constant results and possible residual defects. These drawbacks are critical in applications like running blades, where precision and repeatability are essential. For these reasons, the Prepreg-Vacuum Bagging process was considered as the best option, allowing precise control of fiber orientation and resin ratio, improved part quality and better mechanical consistency, all while being cost-effective.
If we consider that the "Cheetah Xtreme" model costs around 15000€, and assume a mark up of 5x, the company's costs could be approximately 3000€. This is a very high value compared to the cost we estimated for raw materials alone, but it is fully justifiable since, in our estimate, we did not took account several other components actually present, such as metal inserts to attach the blade to the socket, production costs, high customization and optimization for each athlete, high-end raw materials, mandatory certification tests required by regulations, and also the costs associated with the brand name.

2.5 Conclusions

In conclusion, the simulation results led to the following results:

- The analytical analysis previously carried out is consistent with the numerical simulation, identifying the "S"-shaped region of the blade as the most critical area.
- Both composite materials exhibit no issues with respect to structural integrity: 28 and 44 plies are required for CFRP and GFRP blades, respectively, to withstand a load of $2000\,N$. Furthermore, a comparison between stacking configurations with and without 90° oriented plies revealed that the inclusion of 90° plies is detrimental, as it increases the number of layers required to meet both failure and displacement criteria.
- To achieve a vertical displacement of $4\,cm$ at the tip of the foot, the CFRP blade requires 52 plies, while the GFRP blade needs 84. This makes CFRP the preferred material, ensuring better performance by

reducing the inertial mass of the component. However, the weight of our blade of $1.75\,kg$ is far from the one specified from Össur, that is $1\,kg$, resulting in a $43\,\%$ difference: we believe that this difference comes from several factors that we neglected for simplicity, such as the plies thickness optimisation and the change in the number of plies.

- Metallic materials, including the lightest alloys, proved to be less efficient than CFRP, with simulated weight increase of approximately 37.5%. On the other hand, the AA7075 satisfied the displacement constraint with a lower weight with respect to GFRP: however, in the market, aluminium made prosthesis are not available. This can be linked to different reasons, for example corrosion-related degradation does not affect composite blades, making them way more durable. Moreover, for our application, CFRP provides a sensible improvement in performances, making the choice of other materials not recommended.
- The process that represents the best compromise in terms of personalization, finishing and cost-effectiveness is the Prepreg-Vacuum Bagging.

References

[1] Saleel Hussein Abood and Majid Habeeb Faidh-Allah. "Analysis of Prosthetic Running Blade of Limb Using Different Composite Materials". In: *Journal of Engineering* 25.12 (Dec. 2019), pp. 15–25. ISSN: 1726-4073. DOI: 10.31026/j.eng.2019.12.02.

[2] Yasser Alizadeh and Thermo Fisher Scientific. "Design and Structural Analysis of Composite Prosthetic Running Blades for Athletes: A case of dynamic explicit analysis using Abaqus CAE". In: (). DOI: 10.13140/RG.2.2.20693.04327. URL: https://www.researchgate.net/publication/342336561.

[3] Ahmed Samir Ead et al. *Life cycle analysis for green composites: A review of literature including considerations for local and global agricultural use*. 2021. DOI: 10.1177/15589250211026940.

[4] Gianmario Foscan. *UNIVERSITÀ DEGLI STUDI DI PADOVA*. Tech. rep.

[5] Khairul Izwan Ismail, Tze Chuen Yap, and Rehan Ahmed. *3D-Printed Fiber-Reinforced Polymer Composites by Fused Deposition Modelling (FDM): Fiber Length and Fiber Implementation Techniques*. Nov. 2022. DOI: 10.3390/polym14214659.

[6] L Limmer et al. *The potential of 3-D woven composites exemplified in a composite component for a lower-leg prosthesis*. Tech. rep. 1996, pp. 21–217.

[7] Dipen Kumar Rajak et al. "Recent progress of reinforcement materials: A comprehensive overview of composite materials". In: *Journal of Materials Research and Technology* 8.6 (Nov. 2019), pp. 6354–6374. ISSN: 22387854. DOI: 10.1016/j.jmrt.2019.09.068.

[8] Md Irfanul Haque Siddiqui et al. "Static Behavior of a Prosthetic Running Blade Made from Alloys and Carbon Fiber". In: *Journal of Disability Research* 2.1 (2023). ISSN: 26762633. DOI: 10.57197/jdr-2023-0010.